Takeshi Kunitomo, Hamdy M. Shafey

RADIATIVE HEAT TRANSFER IN THE Na MIST DISPERSION OVER THE HOT SURFACE OF LIQUID Na IN THE COOLING SYSTEM OF NUCLEAR REACTOR

Department of Engineering Science, Kyoto University, Kyoto, Japan

1. Introduction

Radiative transfer in a scattering medium plays an important role in many problems of heat transfer. In the present study the analysis is carried out for the practical engineering system of the Na mist particles dispersed in the Ar cover gas enclosed by the hot specular surface of liquid Na from the lower side and by the cold diffuse surface of a solid plate from the upper side in the cooling system of nuclear reactor. The medium of the Na mist dispersion is considered to be nonisothermal, nongray, and with plane parallel geometry. The Na mist emits, absorbs and anisotropically scatters radiation energy. The boundaries are considered to be emitting and reflecting. The temperature variation gives rise to an inhomogeneity in the scattering and absorption properties of the dispersing medium through the variation of the volume concentration of the mist particles and the temperature dependence of the optical constants of liquid Na. The analysis is based on replacing the inhomogeneous dispersing medium by three discrete homogeneous layers, and formulating the transfer equation for the monochromatic radiation in each layer according to Chandrasekhar's theory. The scattering contribution to the transfer equation for each layer is described by a scattering albedo of the layer and a corresponding phase function. These properties are calculated for the spherical particles of Na mist from the equations of Mie theory. The Gaussian quadrature formula is used for replacing the integrals in the transfer equations or the boundary conditions, by the corresponding summations. The Gaussian elimination method is applied to obtain the constants of the numerical solutions of the resulting linearly independent first order differential equations subjected to the conditions at the outer and internal boundaries between the layers. The

numerical results of the integrated net radiative flux are obtained by considering stepwise variation of the spectral properties of the dispersing medium and the boundaries, and integrating numerically over the wavelength range of interest using a finite number of wavelength intervals. The radiative heat flux is compared with the convective heat flux.

2. Mathematical Formulation

2.1 Theoretical Model and Assumptions

The model selected for the present study represents the Na mist formed in the Fast Breeder Reactor in which the condensed liquid particles are dispersed in the mixture of the Ar cover gas and the Na vapor. Fig.1 shows the theoretical model in which the Na mist dispersion of thickness L is enclosed between the hot specular surface of liquid Na at a temperature T_H and the cold diffuse surface of the Na deposit at a temperature T_C. The mist dispersion is divided into three homogeneous layers which may be representative to the actual conditions considering the other modes of heat and mass transfer. We consider the following for the analysis of the radiative transfer.

(1) For the calculation of radiative transfer, the temperatures of the upper and lower boundary layers can be represented by the average temperatures, respectively, while the intermediate layer represents the region of a uniform temperature T_G.

(2) The liquid Na particles absorb, emit and anisotropically scatter radiation energy while the medium (Ar and Na vapor) does not react with it and its refractive index is unity.

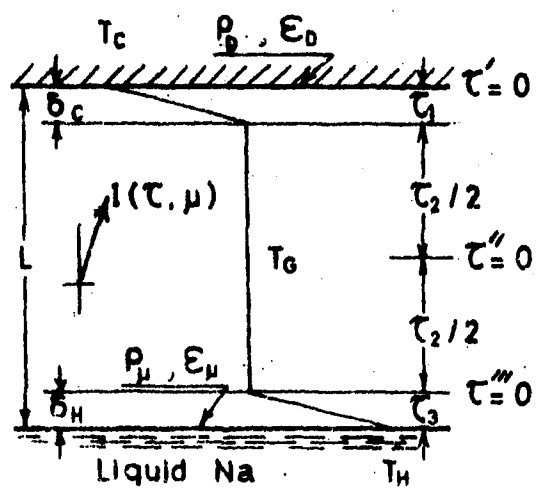

Fig.1 Theoretical model of the Na mist dispersion

(3) The system is assumed to be plane parallel with one dimensional radiative transfer and in the steady state condition.

(4) The local thermodynamic equilibrium exists for each layer.

2.2 Radiative Transfer Equation

The equation governing

the transfer of the monochromatic radiation within each layer can be expressed by

$$\mu \frac{dI_{1,2,3}(\tau,\mu)}{d\tau} = I_{1,2,3}(\tau,\mu) - \frac{\tilde{\omega}_{1,2,3}}{4\pi} \int_{4\pi} p_{1,2,3}(\cos\Theta) I_{1,2,3}(\tau,\mu') d\Omega' - (1-\tilde{\omega}_{1,2,3}) I_{b1,2,3}(\tau) \quad , \tag{1}$$

where the numbers 1,2,3 donote the upper, intermediate and lower layers, respectively, with τ representing the optical depth τ', τ'', τ''' and given by

$$\tau = \int_0^z K_e dz \quad . \tag{2}$$

The scattering albedos $\tilde{\omega}_{1,3}$ for the upper and lower layers are obtained as the average values and given by

$$\tilde{\omega}_1 = \int_{T_C}^{T_G} K_s dT / \int_{T_C}^{T_G} K_e dT \quad , \quad \tilde{\omega}_3 = \int_{T_G}^{T_H} K_s dT / \int_{T_G}^{T_H} K_e dT \tag{3}$$

and $$K_s = \frac{1.5}{d} \cdot X_{sp} \cdot v \quad , \quad K_e = \frac{1.5}{d} \cdot X_{ep} \cdot v \tag{4}$$

where v is the local mist volume concentration. The scattering albedo $\tilde{\omega}_2$ is given by

$$\tilde{\omega}_2 = X_{sp}(T_G)/X_{ep}(T_G) \quad . \tag{5}$$

X_{sp} and X_{ep} are the scattering and extinction efficiency factors for single liquid Na particle of diameter d and can be calculated by the Mie theory.[1] The scattering phase function $p_{1,2,3}(\cos\Theta)$ is expressed in a series expansion of Legendre polynomials as[1]

$$p_{1,2,3}(\cos\Theta) = \sum_{k=0}^{N} C_{k1,2,3} P_k(\cos\Theta) \quad , \tag{6}$$

where the angular distribution coefficients $C_{k1,2,3}$ are given by

$$C_{k1} = \{C_k(T_C)+C_k(T_G)\}/2 \quad , \quad C_{k2} = C_k(T_G) \quad , \quad C_{k3} = \{C_k(T_G)+C_k(T_H)\}. \tag{7}$$

The monochromatic blackbody intensities $I_{b1,3}(\tau)$ for the upper and lower layers are assumed to be constant and given by

$$I_{b1} = \int_{T_C}^{T_G} K_a I_b(T) dT / \int_{T_C}^{T_G} K_a dT \quad , \quad I_{b3} = \int_{T_G}^{T_H} K_a I_b(T) dT / \int_{T_G}^{T_H} K_a dT \tag{8}$$

where the local absorption coefficient K_a is given by

$$K_a = K_e - K_s \quad . \tag{9}$$

2.3 Numerical Solution

Substituting Eq.(6) in Eq.(1) and applying the Gaussian

quadrature formula, we obtain (without the layer notation)

$$\mu_i \frac{dI(\tau,\mu_i)}{d\tau} = I(\tau,\mu_i) - \frac{\tilde{\omega}}{2} \sum_{j=1}^{2n} w_j G_{ij} I(\tau,\mu_j) - (1-\tilde{\omega}) I_b(\tau) \quad , \qquad (10)$$

$$(i=1,2,\cdots,2n)$$

$$\text{where} \quad G_{ij} = \sum_{k=0}^{N} C_k P_k(\mu_i) P_k(\mu_j). \qquad (11)$$

The solution to the system of equations in Eq.(11) can be expressed by

$$I(\tau,\mu_i) = \sum_{\alpha=1}^{2n} g_\alpha b_{i\alpha} e^{\gamma_\alpha \tau} + I_b \quad (i=1,2,\cdots,2n) \quad , \qquad (12)$$

where the constants γ_α and $b_{i\alpha}$ are obtained for each layer as the eigen values and eigen vectors of the 2n linearly independent algebraic equations resulting from the substitution of the solution $be^{\gamma\tau}$ in the homogeneous system of Eq.(10), and I_b is the particular solution. The constants of integration for each layer $g_{\alpha 1,2,3}$ are obtained by the Gaussian elimination method applied to the equations resulting from the substitution of the numerical solution $I_{1,2,3}(\tau,\mu_i)$ in the numerical form of the boundary and continuity conditions defined by the following equations.

$$\text{At} \quad \tau' = 0 \; : \; I_1(0,-\mu) = J_C/\pi \quad , \qquad (13)$$

where J_C is the monochromatic radiosity at the cold surface and is given by

$$J_C = \varepsilon_D \pi I_b(T_C) + \rho_D \int_{2\pi} I(0,\mu)\mu d\Omega \quad . \qquad (14)$$

Replacing the integration in Eq.(14) by the corresponding Gaussian formula, Eq.(14) can be written as

$$I_1(0,-\mu) = \varepsilon_D(T_C) \cdot I_b(T_C) + 2\rho_D(T_C) \sum_{j=1}^{n} w_j \mu_j I_1(0,\mu_j) \quad . \qquad (15)$$

$$\text{At} \quad \tau' = \tau_1 \; , \; \tau'' = -\tau_2/2 \; : \; I_1(\tau_1,\pm\mu) = I_2(-\tau_2/2,\pm\mu). \qquad (16)$$

$$\text{At} \quad \tau'' = \tau_2/2 \; , \; \tau'' = 0 \; : \; I_2(\tau_2/2,\pm\mu) = I_3(0,\pm\mu) \; . \qquad (17)$$

$$\text{At} \quad \tau''' = \tau_3 \; : \; I_3(\tau_3,\mu) = \varepsilon_\mu(T_H) \cdot I_b(T_H) + \rho_\mu(T_H) I_3(\tau_3,-\mu). \qquad (18)$$

In the above equations τ_1, τ_2 and τ_3 are given by

$$\tau_1 = \int_0^{\delta_C} K_e dz \quad , \quad \tau_2 = K_e(T_C)(L-\delta_C-\delta_H) \text{ and } \tau_3 = \int_0^{\delta_H} K_e dz \, . \qquad (19)$$

The specular reflectivities $\rho_\mu(T_H)[\equiv 1-\varepsilon_\mu(T_H)]$ are calculated by Fresnel's formula. The hemispherical diffuse reflectance $\rho_D(T_C)[\equiv 1-\varepsilon_D(T_C).]$ is assumed to be equal to the hemispherical specular reflectance (for diffuse irradiation).

3. Optical Constants of the Liquid Na

For the wavelength range of interest in the present study (λ = 1.6∿30 μm) the optical constants (n, k) of liquid Na can be determined from the classical Drude equation[2], by solving the following equations.

$$n^2-k^2 = 1-\sigma_{dc}\frac{4\pi\tau^*}{(1+\omega^2\tau^{*2})}\ ,\quad nk = \sigma_{dc}\frac{2\pi}{\omega(1+\omega^2\tau^{*2})}\ ,$$
$$\tau^* = \sigma_{dc}\cdot\frac{m^*}{n^*e^2}\ , \tag{20}$$

where m* is given as 1.17 m_e (m_e is the mass of the electron). The dc electrical conductivity σ_{dc} is calculated from the measurement of the dc electrical resistivity on the liquid Na over the temperature range 133∿1087°C, and the number density n* is also given as the function of the temperature[3].

4. The Na Mist Concentration

The calculation of the local mist volume concentration v at a temperature T is based on the simple assumption of the local equilibrium condensation of the saturated Na vapor at the temperature T_H of the hot liquid Na surface to the saturated liquid and vapor at the considered temperature T. It may be given by

$$v(T) = [\frac{1}{v_s(T_H)} - \frac{1}{v_s(T_C)}]/\rho_l(T)\ , \tag{21}$$

where $v_s(T_H)$ and $v_s(T_C)$ are the specific volumes of the saturated Na vapor at T_H and T_C. These values are obtained by the equations recommended in Ref.(3).

5. Analysis of The Calculated Results

The integrated net radiative fluxes $q_r(T_C)$ and $q_r(T_H)$ at the cold and hot surfaces, respectively, are given by

$$q_r(T_C) = \int_0^\infty F_1(0)d\lambda \cong \int_{\lambda_1}^{\lambda_2} F_1(0)d\lambda \cong \sum_{i=1}^{M} F_1(0,\lambda_i)\Delta\lambda_i$$
$$\text{and}\quad q_r(T_H) \cong \sum_{i=1}^{M} F_3(\tau_3,\lambda_i)\Delta\lambda_i\ , \tag{22}$$

where the monochromatic net radiative flux $F_{1,3}(\tau)$ can be given numerically by

$$F_{1,3}(\tau) = 2\pi\sum_{j=1}^{2n} w_j\mu_j I_{1,3}(\tau,\mu_j)\ , \tag{23}$$

and λ_1 and λ_2 are the lower and upper limits of the wavelength range.

The convective heat fluxes $q_c(T_C)$ and $q_c(T_H)$ for natural convection by Ar gas are calculated by

$$q_c(T_C) = h_C(T_G - T_C) \quad , \quad q_c(T_H) = h_H(T_H - T_G), \tag{24}$$

where h_C and h_H are the heat transfer coefficients and given by[4]

$$h_{C,H} = 0.17\, k^*_{C,H} \left\{\frac{g\beta_{C,H}(T_{C,H} - T_G)}{\nu^2}\right\}^{1/3} p_r^{0.407}. \tag{25}$$

In the calculation, the arithmetic mean temperature of T_C and T_H is first given to T_G and the iteration is carried out, by changing T_G slightly, to fulfill the total heat balance equation,

$$q_c(T_C) + q_r(T_C) = q_c(T_H) + q_r(T_H) \quad . \tag{26}$$

6. Results and Discussions

A computer program was prepared to perform the above mentioned mathematical procedure numerically and the input data were selected to be representative for the condition met in the application of sodium cooled fast breeder reactor. The variety in such conditions assording to the power requirement is corsidered in the study of the effects of T_H, T_C, L and d on the final results.

Shown in Figs.2∿5 are the results for the average fluxes q_r, q_c and the total fluxes. Figure 2 shows the effect of T_C. All fluxes decrease with the increase in T_C, but q_c decreases by a higher rate. For small values of T_C, q_c is larger than q_r while they are equal at $T_C \cong 350°C$ and q_r is larger than q_c at a higher T_C. In all cases q_r has the same order of q_c and the neglection of the radiative flux q_r in the treatment of the heat transfer in the Na mist layer leads to a serious error. Figure 3 shows the effect of T_H. Both q_c and q_r increase nearly by the same rate with the increase in T_H, and thus the total flux increases nearly by a double rate more than q_c and q_r. The convective flux is always larger than the radiative flux for the conditions of T_C selected here. It must be noticed that the other values for T_C may result in a condition where q_r is larger than q_c as shown in Fig.2. The broken lines in Figs. 2 and 3 denote the radiative fluxes calculated by the approximate formula for the case of two infinite plane parallel gray surfaces at the temperatures T_H and T_C with perfectly transparent medium. As shown the approximate

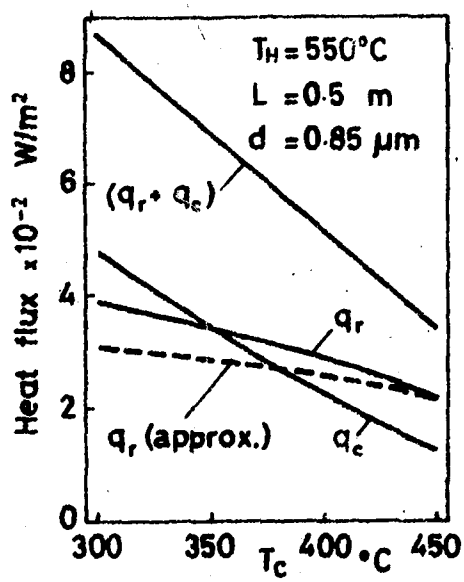

Fig.2. Effect of T_C on radiative, convective and total fluxes

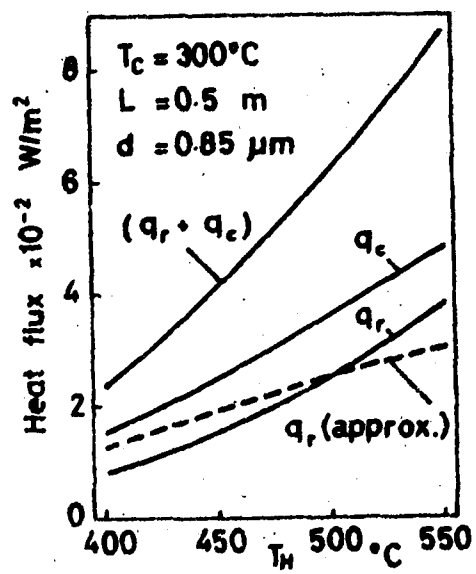

Fig.3. Effect of T_H on radiative, convective and total fluxes

formula underestimates for the large temperature difference while it gives equal or larger values for the smaller temperature difference.

Figure 4 shows the effect of L. The slight decrease is found in all fluxes with the increase of L. This is due to the mechanism of multiple scattering, absorption and reemission with the mist layer which may affect much the spatial distribution of the radiative flux inside the mist layer while it has no considerable effect at the boundaries which are affected much by the temperatures T_H and T_C.

Figure 5 shows the effect of the particle diameter of the Na mist. The values for d are chosen to represent the possible deviations around the average value of 0.85 μm. The flux q_r is nearly constant and the diameter has negligible effect on it. Therefore the uncertainty in the value of d in the range selected here does not lead to a considerable error in the calculation of the heat transfer in the Na mist layer.

7. Conclusions

The analysis has been carried out for the radiative transfer in the Na mist dispersion enclosed between the hot surface of the liquid Na and the cold surface of Na deposit. The summary of the results is shown below.

(1) The radiative flux has the same order of the convective flux for all conditions of the Na mist dispersion.

(2) Both radiative and convective fluxes increase by nearly equal

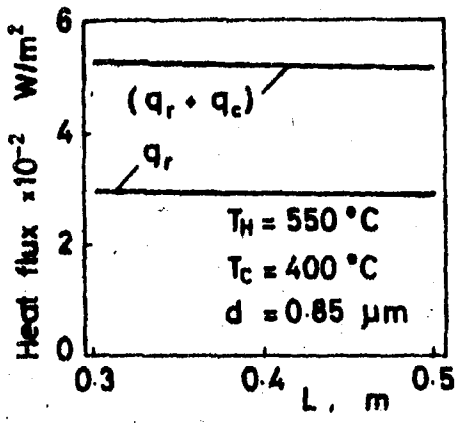

Fig.4. Effect of L on radiative and total fluxes

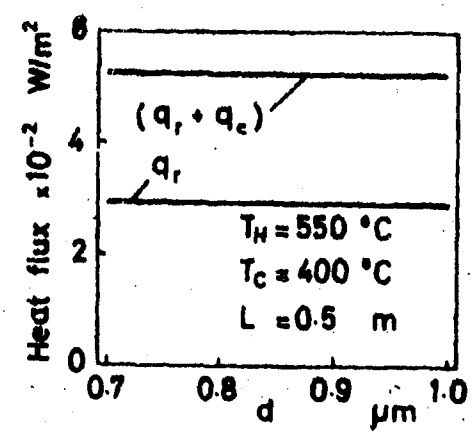

Fig.5. Effect of d on radiative and total fluxes

rates with the increase of the temperature T_H and decrease by the different rates with the increase of T_C.

(3) The allowed uncertainty selected here in the value of the particle diameter of the Na mist does not lead to a considerable error in the calculation of the radiative flux.

(4) The radiative and total fluxes decrease slightly with the increase in the total thickness of the Na mist dispersion.

(5) The approximate calculation underestimates the radiative flux for the large temperature difference.

Nomenclature

$b_{i\alpha}$- constant; C_k- angular distribution coefficient;

d- diameter of liquid Na particle(m)

F- net flux of the monochromatic radiation(w/m^3);

g- gravitational acceleration(m/s^2);

g_α- constant;

h- heat transfer coefficient by free convection($w/m^2 \cdot °C$);

I- monochromatic intensity($w/m^3 \cdot sr$);

J- monochromatic radiosity(w/m^3);

K_s, K_a and K_e- scattering, absorption and extinction coefficients of the layer for single scattering(m^{-1});

k- imaginary part of the complex refractive index;

k*- thermal conductivity of Argon gas($w/m \cdot °C$);

L- total space length(m); $p(\cos\Theta)$- scattering phase function;

p_k- Legendre polynomial of an order k;

q_c- convective heat flux(w/m^2);

q_r- radiative heat flux(w/m^2); T- temperature(°C);

v- local mist volume concentration; w_j- Gaussian weight;

v_s- specific volume of saturated Na vapor(m^3/kg);
X_{sp}, X_{ep}- scattering and extinction efficiency factors for single scattering; ν- kinematic viscosity of Argon gas(m^2/s);
γ_α- constant; δ- boundary layer thickness(m);
ε_μ, ε_D- directional emissivity and hemispherical emittance;
λ- wavelength in the vacuum(μm); μ- cosine of the polar angle;
μ_j- Gaussian division according to the zeros of $p_{2n}(\mu)$;
Θ- angle between μ and μ';
ρ_μ, ρ_D- directional specular reflectivity and hemispherical diffuse reflectance; ρ_e- density of saturated liquid Na(kg/m^3);
σ_{dc}- dc electrical conductivity of liquid Na(S/m);
τ- normal optical depth; τ^*- relaxation time(s);
ω- angular frequency of light(rad/s);
$\tilde{\omega}$- scattering albedo of the layer for single scattering.
Subscripts 1, 2, 3- upper cold boundary layer, main flow layer, lower hot boundary layer; C- relating to the cold surface; b- blackbody; H- relating to the hot liquid Na surface.

References

1. T. Kunitomo, H. M. Shafey and T. Teramoto. "Theoretical Study on Radiative Properties of a Painted Layer Containing Spherical Pigment(Case of Normal Incidence)", Bulletin of JSME, Vol.22, No.173(1979), p.1587.
2. T. Inagaki, E. T. Arakawa, R. D. Birkhoff and M. W. Williams. "Optical properties of liquid Na between 0.6 and 3.8 eV", Phys. Review B, Vol.13, No.12(1976), p.5610.
3. G. H. Golden and J. V. Tokar . "Thermophysical Properties of Sodium", ANL-7323(1967).
4. I. Kudo and M. Hirata. "Study on Na Deposition on Parallel Plate Opposite to Liquid Na Surface(2nd Report)", Trans. of JSME, Vol.43, No.368(1977), p.1407.